Journal of Mathematical Chemistry, Vol. 39, No. 1, January 2006 (© 2005)
DOI: 10.1007/s10910-005-9006-4

Modeling isothermal free-radical frontal polymerization with gel effect using free volume theory, with and without inhibition

D.E. Devadoss and V.A. Volpert*

Department of Engineering Sciences and Applied Mathematics, Northwestern University, 2145 Sheridan Rd., Evanston, IL 60208-3125, USA
E-mail: v-volpert@northwestern.edu

Received 29 July 2004; revised 28 September 2004

Frontal Polymerization is a process that converts monomers into polymers by means of a propagating spatially localized reaction front. Such fronts exist with free-radical polymerization, where in the simplest case, a mixture of monomers and initiator is placed into a test tube and upon initiation of the reaction at one end of the tube, a self-sustained wave develops and propagates through the tube. Isothermal Frontal Polymerization (IFP), often referred to as interfacial gel polymerization, occurs due to the coupling of mass diffusion of the species and the gel effect. Utilizing the free volume theory of Vrentas and Duda for describing the self-diffusive behavior of the gel effect, we mathematically model and study this IFP process. We determine, both numerically and analytically, characteristics of the process including the propagation velocity of the reaction zone, the structure of the wave, and the distance traveled by the front before it breaks down due to reactions ahead of the front.

KEY WORDS: polymerization, mathematical modeling, isothermal frontal polymerization, gel effect

AMS classification: 35K57, 80A30, 60J60

1. Introduction

Frontal polymerization is a process that converts monomers into polymers by means of a self-propagating wave. This front is a highly localized spatial reaction zone which propagates through a mixture of monomers and initiator, leaving polymers in its wake.

*Corresponding author.

The chemical mechanism for FP is usually free-radical polymerization, which in the simplest case includes three kinetic steps: initiation, propagation, and termination.

There are two modes of frontal polymerization: isothermal and thermal. Thermal frontal polymerization is usually initiated by applying a heat source at one end of a test tube. The temperature increase induces decomposition of the initiator into active radicals allowing polymer chain growth to begin. The chain growth, which occurs in a narrow region with sufficiently high temperature, releases more heat which diffuses into an adjacent layer of reactants inducing decomposition of initiator there. In this way, a self-sustained reaction wave can travel through the mixture. The increase in temperature can be as high as 200 K. The propagation of the wave is hence due to the exothermic chemical reactions and heat diffusion. A review of experimental and theoretical works on thermal frontal polymerization can be found in [1].

In an isothermal mode of polymerization, the propagation of the wave is due to the mass diffusion of the species and the gel effect. The reaction typically starts when a polymer seed, that is, a piece of polymer, is placed in contact with a solution of its monomer and an initiator. The monomer swells the seed and the gel region is formed. Polymerization occurs faster in the swelled viscous gel than in the more fluid bulk medium. This causes the termination rate to severely diminish. The result is an acceleration in the overall rate of polymerization and hence an increase in the conversion of monomers. This phenomenon is called the gel effect. Mass diffusion supplies the monomer molecules to the growing gel region.

Often, due to the gel effect, the front is prevented to propagate due to increased bulk polymerization. By adding a small but effective amount of inhibitor, the radicals can also react with the inhibitor molecules. When this occurs, the polymerization reaction is terminated. Inhibitors stop every radical, and polymerization is almost completely halted until the inhibitors are consumed. Hence the front has the chance to propagate longer before bulk polymerization causes its breakdown. It would be ideal to use an inhibitor that works in the bulk but does not significantly penetrate into the gel region.

Theoretical and experimental studies of isothermal frontal polymerization have been performed in [2–12].

In this paper we consider a system that exhibits strong gel effect [13]. That is, a system that leads to a nonideal behavior of drastically increasing polymerization in the bulk. A classical example of such a system is with methyl methacrylate (MMA) as the monomer, 2,2-azobisbutronitrile (AIBN) as the initiator, and polymethyl methacrylate (PMMA) as the resulting polymer. (Poly)vinyl phenol is often used as the inhibitor.

2. Mathematical model

2.1. Basic mechanism

The following kinetic scheme summarizes the three basics steps (initiation, propagation, termination) of free-radical polymerization [14]:

$$\text{Initiation} \begin{cases} I \xrightarrow{k_d} f\, 2R\cdot \\ R\cdot + M \xrightarrow{k_i} P_1\cdot \end{cases}$$

$$\text{Propagation} \begin{cases} P_1\cdot + M \xrightarrow{k_p} P_2\cdot \\ P_2\cdot + M \xrightarrow{k_p} P_3\cdot \\ \cdots \\ P_j\cdot + M \xrightarrow{k_p} P_{j+1}\cdot \\ \cdots \end{cases}$$

$$\text{Termination} \left\{ P_n\cdot + P_m\cdot \xrightarrow{k_{tg}} P \right.$$

In the above, I is the initiator species, $R\cdot$ is the primary radical, M is the monomer species, $P_j\cdot$ is the polymer radical of length j, and the chemically inactive polymer is P. All chemically active species are denoted with a dot besides them. The term f is the efficiency of the initiator and typically has the value of 0.5. The radicals are highly reactive and only a fraction of those formed by decomposition are consumed by combination to monomer [13]; f is defined as the quotient of $R\cdot$ that successfully initiate chains to the total $R\cdot$ formed.

The reaction rate constants, k_j, depend on temperature of the system and are written in the Arrhenius form as

$$k_j = k_j^o \exp\left(-\frac{E_j}{R_g T}\right) \quad \text{for } j = d, i, p, tg,$$

where k_j^o is the frequency factor, E_j is the activation energy, and R_g is the universal gas constant. Though there is net heat production in the system, we assume that the temperature T is constant due to efficient heat removal by heat losses to the environment. Indeed, this assumption is accurate because the IFP process is extremely slow; the propagation velocity of the front is of the order of 1 cm/day. Thus, the decomposition, initiation, and propagation rate parameters, k_d, k_i, and k_p, respectively, are constant [13]. The termination rate parameter k_{tg} is not constant; it is a function of the degree of conversion of the monomer. The termination rate parameter models the gel effect as discussed later.

2.2. Approximations and governing equations

We develop a one dimensional model of IFP. For the spatial region we consider the interval $0 < \tilde{x} < L$, where L is the length of the tube along which the front propagates.

The following system of equations describe the change in the concentration of the species at time $\tilde{t}$. The tilde denotes dimensional quantities.

$$\frac{d\tilde{I}}{d\tilde{t}} = -k_d \tilde{I} \tag{1a}$$

$$\frac{d\tilde{R}\cdot}{d\tilde{t}} = 2fk_d \tilde{I} - k_i \tilde{M}\tilde{R}\cdot \tag{1b}$$

$$\frac{d\tilde{M}}{d\tilde{t}} = -k_i \tilde{M}\tilde{R}\cdot - k_p \tilde{M}\tilde{P}\cdot \tag{1c}$$

$$\frac{d\tilde{P}\cdot}{d\tilde{t}} = k_i \tilde{M}\tilde{R}\cdot - 2k_{tg}\tilde{P}\cdot^2 \tag{1d}$$

$$\frac{d\tilde{P}}{d\tilde{t}} = k_{tg}\tilde{P}\cdot^2 \tag{1e}$$

To describe the means of propagation in an isothermal system in entirety, both mass diffusion of the species and gel effect must be included. Thus, we include a diffusion term into equation (1c) to obtain

$$\frac{\partial \tilde{M}}{\partial \tilde{t}} = D_M \frac{\partial^2 \tilde{M}}{\partial \tilde{x}^2} - k_i \tilde{M}\tilde{R}\cdot - k_p \tilde{M}\tilde{P}\cdot, \tag{2}$$

where the diffusion coefficient, D_M, is taken to be constant. This model does not account for the diffusion of the other species. Indeed, assuming that it is uniformly distributed at the initial time, the initiator remains so at all times, and thus we do not need to include a diffusion term in (1a). Next, the lifetime of the primary radicals is relatively short and hence their diffusion is assumed negligible. We also neglect the diffusion of the larger molecules, namely the polymer radicals and dead polymers, since such molecules diffuse very slowly relative to the smaller monomer molecules.

To simply the analysis of the problem, we reduce the number of reaction rate parameters in the problem by assuming $k_i = k_p$, an approximation justified in [15]. As the concentration of $\tilde{R}\cdot$ is known to be much less than of $\tilde{P}\cdot$ [15], we sum equations (1b) and (1d), introduce a combined concentration of chemically active radicals, $D = \tilde{R}\cdot + \tilde{P}\cdot$, and apply the assumption $\tilde{R}\cdot \ll \tilde{P}\cdot$.

To complete the formulation of the problem, we state the appropriate initial and boundary data. Before initiation, there are no radical or polymer molecules in the system and hence their initial concentrations is zero. The initial concentrations of the initiator and monomer will be denoted by I_o and M_o, respectively.

To initiate the reaction, we assume a polymer seed is placed at one end of the tube ($\tilde{x} = 0$). To this end, we fill in the region $0 < \tilde{x} < x_o$ with a polymer substrate which is free of monomer, while the remaining part $x_o < \tilde{x} < L$ of the initial mixture is filled with initiator and monomer. After initiation, the reaction wave propagates toward the other end of the tube ($\tilde{x} = L$) where we impose a no-flux boundary condition on M.

Upon enforcing the above assumptions, the system of equations takes the form

$$\frac{\partial \tilde{I}}{\partial \tilde{t}} = -k_d \tilde{I}, \tag{3a}$$

$$\frac{\partial \tilde{D}}{\partial \tilde{t}} = 2 f k_d \tilde{I} - 2 k_{tg} \tilde{D}^2, \tag{3b}$$

$$\frac{\partial \tilde{M}}{\partial \tilde{t}} = D_M \frac{\partial^2 \tilde{M}}{\partial \tilde{x}^2} - k_p \tilde{D} \tilde{M}, \tag{3c}$$

$$\frac{\partial \tilde{P}}{\partial \tilde{t}} = k_{tg} \tilde{D}^2, \tag{3d}$$

subject to initial conditions

$$\tilde{I}(\tilde{x}, 0) = I_o, \quad \tilde{M}(\tilde{x}, 0) = M_o \cdot H(\tilde{x} - x_o) \equiv \begin{cases} M_o & \text{if } \tilde{x} > x_o \\ 0 & \text{if } \tilde{x} < x_o \end{cases}, \quad \tilde{D}(\tilde{x}, 0) = 0, \quad \tilde{P}(\tilde{x}, 0) = 0, \tag{4}$$

and boundary conditions

$$\tilde{M}(0, \tilde{t}) = 0, \quad \frac{\partial \tilde{M}(L, \tilde{t})}{\partial \tilde{x}} = 0. \tag{5}$$

We make two further observations to clarify the problem. First, notice that equation (3d) decouples from the remaining equations. Thus we restrict ourselves to a study of equations (3a)–(3c), while $\tilde{P}$, if needed, can be easily calculated once $\tilde{D}$ is determined. Finally, equation (3a), subject to the initial condition in (4) can be solved explicitly to give

$$\tilde{I} = I_o \mathrm{e}^{-k_d \tilde{t}}.$$

This reduces our problem to two coupled equations and corresponding data:

$$\frac{\partial \tilde{D}}{\partial \tilde{t}} = 2 f k_d I_o \mathrm{e}^{-k_d \tilde{t}} - 2 k_{tg} \tilde{D}^2, \tag{6}$$

$$\frac{\partial \tilde{M}}{\partial \tilde{t}} = D_M \frac{\partial^2 \tilde{M}}{\partial \tilde{x}^2} - k_p \tilde{D} \tilde{M}, \tag{7}$$

$$\tilde{D}(\tilde{x}, 0) = 0, \quad \tilde{M}(\tilde{x}, 0) = M_o \cdot H(\tilde{x} - x_o), \quad \tilde{M}(0, \tilde{t}) = 0, \quad \frac{\partial \tilde{M}(L, \tilde{t})}{\partial \tilde{x}} = 0. \tag{8}$$

2.3. Gel effect

As the concentration of polymer chains in solution increases in the course of reaction, the viscosity of the system increases. As a result, the long growing chains find it difficult to find other long radicals to terminate, but they can more easily find small monomers to continue to grow. This causes the termination rate to drastically diminish. The outcome is a sharp increase in the overall polymerization rate and hence the sudden increase in the conversion of monomers. This phenomenon is known as the gel effect (also referred to as the Trommsdorff–Norrish effect and autoacceleration effect). The gel effect can hence be described in terms of the dependence of the rate of the termination reaction on the monomer consumption.

Thus, in order to complete the formulation of our problem, we mathematically model the gel effect with the use of the termination rate parameter k_{tg}. Consider interaction of two polymer radical species resulting in a termination reaction. The radicals need to diffuse to within a reaction distance from one another for termination to occur. The diffusion process can be described in the framework of the self-diffusion theory. This theory discusses, in particular, the diffusion of polymer chains in a mixture of polymer and monomers, with a dependence on the concentration of polymers. This theory [13] gives the following expression for the termination rate parameter

$$k_{tg} = k_t^o \left[\frac{D_m(c)}{D_{mo}} \right]^{\beta_*} \tag{9}$$

In the above, $D_m(c)$ is the polymer self-diffusion rate which depends on the polymer concentration c, with $D_{mo} \equiv D_m(0)$. The constant k_t^o is the termination rate coefficient, and β_* is a parameter which is associated with the length of the polymer radical chains. The longer the chain, the larger is β_*. Experimental data [13, 16] gives a general range of $2 < \beta_* < 10$.

An expression for the polymer self-diffusion rate as a function of temperature and weight fractions of polymers and monomers in a mixture has been derived using the free volume theory [17, 18]. This theory is based on the idea that monomers and polymers can only move through the "free volume" between one another. The rate of self-diffusion can be described using a statistical description of this free volume and is given by D_m:

$$D_m = D_{mo} \cdot \exp\left[- \frac{\Gamma}{\hat{V}_{FH}} \left(\omega_m \hat{V}_m^* + \omega_p \, \xi_{m,p} \hat{V}_p^* \right) \right], \tag{10}$$

where

$$\frac{\hat{V}_{FH}}{\Gamma} = \omega_m \frac{K_{1m}}{\Gamma_m} \left(K_{2m} - T_{gm} + T \right) + \omega_p \frac{K_{1p}}{\Gamma_p} \left(K_{2p} - T_{gp} + T \right). \tag{11}$$

In the above expressions, ω_m and ω_p are the weight fractions of monomer and polymer, respectively. By the definition of weight fraction we have $\omega_m + \omega_p = 1$; for convenience we re-denote $\eta = \omega_p$, and hence $1 - \eta = \omega_m$. The $\hat{V}_m^*$ and $\hat{V}_p^*$ are the specific volumes of the monomer and polymer, respectively, and $\xi_{m,p}$ is the molar size ratio of a monomer molecule to a polymer molecule. Next, $\hat{V}_{FH}$ is the total hole free volume available, and Γ is an overlap value that accounts for the same free volume hole being available to more than one molecule. Also, K_{1m} and K_{2m} are monomer free volume parameters, while K_{1p} and K_{2p} are polymer free volume parameters. The glass transition temperature of the monomer and polymer are T_{gm} and T_{gp}, respectively. The temperature of the system is as before, T. The free volume theory parameters for the PMMA/MMA system are given in table 1. Substituting (10) into equation (9), we obtain

$$k_{tg} = k_t^o \cdot \exp\left[-\beta_* \ \frac{\Gamma}{\hat{V}_{FH}} \left(\omega_m \hat{V}_m^* + \omega_p \ \xi_{m,p} \hat{V}_p^*\right)\right]. \tag{12}$$

Next, we use the parameter values given in table 1 to derive an explicit dependence of the termination rate on η. First we note that equation (11) becomes

$$\begin{aligned}\frac{\hat{V}_{FH}}{\Gamma} &= \omega_m \frac{K_{1m}}{\Gamma_m}\left(K_{2m} - T_{gm} + T\right) + \omega_p \frac{K_{1p}}{\Gamma_p}\left(K_{2p} - T_{gp} + T\right) \\ &= (1-\eta)\,(7.0 \cdot 10^{-4})\,(-32.07 + 300) \\ &\quad +(\eta)\,(3.05 \cdot 10^{-4})\,(-301 + 300) \qquad (13) \\ &\simeq 0.187551\,(1-\eta) \qquad (14)\end{aligned}$$

Here we neglected the second term in (13) as compared to the first term. With the appropriate substitutions, equation (12) can be reduced to

$$k_{tg} = k_t \exp\left[-\frac{\beta}{1-\eta}\right] \tag{15}$$

Table 1
Parameters of the free volume theory for the PMMA/MAA system.

Parameter	Values
$\hat{V}_m^*$	$0.872\,\mathrm{cm^3/g}$
$\hat{V}_p^*$	$0.788\,\mathrm{cm^3/g}$
K_{1m}/Γ_m	$7.0 \cdot 10^{-4}\,\mathrm{cm^3/(K{\cdot}g)}$
K_{1p}/Γ_p	$3.05 \cdot 10^{-4}\,\mathrm{cm^3/(K{\cdot}g)}$
$K_{2m} - T_{gm}$	$-32.07\,\mathrm{K}$
$K_{2p} - T_{gp}$	$-301\,\mathrm{K}$
T	$300\,\mathrm{K}$
$\xi_{m,p}$	0.59

with

$$\beta = 2.5\beta_*, \quad k_t = k_t^o \exp(-2.2\beta_*).$$

3. Nondimensionalization

To solve the problem numerically, we first nondimensionalize the system of equations. We define the nondimensional quantities as

$$D = \frac{\tilde{D}}{D_*}, \quad \eta = \frac{M_o - \tilde{M}}{M_o}, \quad t = \frac{\tilde{t}}{t_*}, \quad x = \frac{\tilde{x}}{x_*}.$$

Note that η, which denoted the weight fraction of polymer, can be readily defined as above. Initially, there is M_o concentration of monomers and no polymers ($\eta = 0$); as time increases and all of the monomers are consumed, the monomer species is fully converted to polymers ($\eta = 1$). Upon substitution of the above and the definition (15) of k_{tg}into equations (6) and (7), we arrive at the following dimensional scales:

$$D_* = \frac{1}{k_p\, t_*}, \quad x_* = \sqrt{D_M t_*}, \quad t_* = \left(\frac{k_t}{2k_p{}^3 f^2 k_d{}^2 I_o{}^2}\right)^{1/4}.$$

In addition, we introduce two small parameters and an inverse of one of them:

$$\varepsilon = k_d t_*, \quad \gamma = \frac{1}{k_p\, t_*{}^2\, 2\, f\, k_d\, I_o}, \quad k \equiv \frac{1}{\gamma}.$$

From equations (6) and (7) and the above definitions, we obtain the following corresponding nondimensional equations

$$\gamma \frac{\partial D}{\partial t} = \mathrm{e}^{-\varepsilon t} - k\mathrm{e}^{-\frac{\beta}{1-\eta}} D^2, \tag{16}$$

$$\frac{\partial \eta}{\partial t} = \frac{\partial^2 \eta}{\partial x^2} + D\,(1-\eta)\,, \tag{17}$$

subject to the initial conditions

$$D(x,0) = 0, \quad \eta(x,0) = H(x_o - x), \tag{18}$$

and the boundary conditions

$$\eta(0,t) = 1, \quad \frac{\partial \eta(L,t)}{\partial x} = 0. \tag{19}$$

Important parameters to keep in mind are γ, k, ε, and β. The numerical values of these parameters depend on the choice of reactants and their kinetic properties. Extensive tabulated values of activation energies, preexponential factors,

and other kinetic parameters for various initiators and monomers can be found in [19].

Equation (16) gives a rate balance of D, the total nondimensional concentration of radicals. In the right hand side of the equation, the first term describes the rate of creation of D (which is equal to the rate of decomposition of the initiator I), and the highly nonlinear second term describes the rate of termination of D. The small magnitude of γ indicates that we will have a stiff problem as it multiplies a time derivative. Equation (17) is an evolution equation for η; there exists a diffusion term and a reaction term. Equations (16)–(19) represent a complete formulation of the nondimensional problem.

4. Results

4.1. Numerical results

The nondimensional system (16)–(19) was solved numerically for several values of β and γ with fixed small parameter ε. As the solution evolves on different timescales (a very fast timescale for D because of the rapid radical–radical reactions and a slower timescale for η), this presents a stiff problem. We used the Method of Lines to obtain a system of ordinary differential equations and solved it using the stiff solver "ode15s" of MATLAB which automatically chooses the appropriate timesteps depending on the stiffness of the problem.

The spatial profiles of the degree of conversion η are shown in figure 1 at equally spaced values of time. A slowly-varying traveling wave is seen. The leftmost curve represents the initial condition imposed on η. As time evolves, we observe a propagating front moving to the right. At any given point on the x-axis, $\eta(x, t)$ moves away from $\eta = 0$ and approaches $\eta = 1$; the product region where $\eta = 1$ grows with time. Even far ahead of the reaction zone, in the bulk region, there is an increase in the conversion of monomer as the front progresses. This eventually causes the breakdown of the front. The solution is slowly-varying since there exist two timescales in the problem: polymerization at the front, where the degree of conversion is high, occurs on a fast time scale, while polymerization in the bulk, where the degree of conversion is relatively small, occurs on a slower time scale.

Figures 2–4 shows various nondimensional plots of the solution to the full problem (equations (16)–(19)) at a fixed time. In particular, figure 2(b) shows the radical concentration profile. Ahead of the front, in the bulk, there is almost no reaction, so only a small quantity of reactive radicals exist and for those present, they are consumed as fast as they are created. But behind the front, there is a much larger concentration of the radicals. This provides testimony to existence of the gel effect. As the reaction progresses, the termination rate drastically diminishes, increasing the radical concentration.

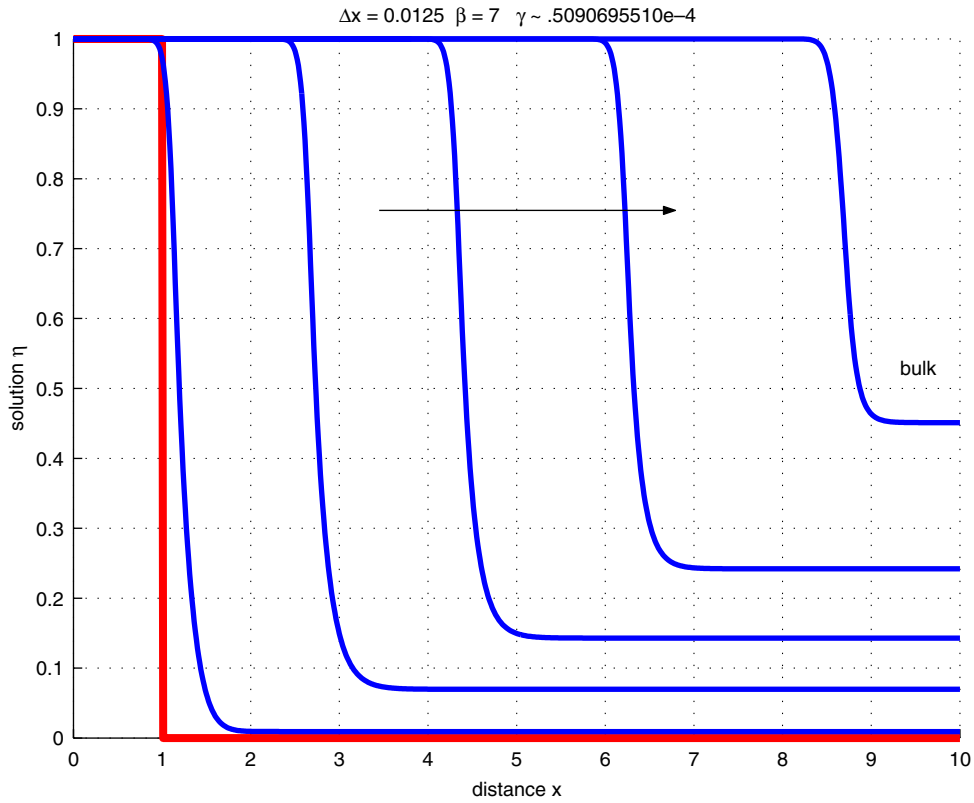

Figure 1. The curves display the spatial profiles of the degree of conversion of the monomer at equally spaced values of time for a reaction without inhibitor.

Table 2 states one set of values that we tested on our model. These parameters are used for all figures unless noted otherwise.

4.2. *Analytical results*

Since the characteristic scale of the reaction zone is much smaller than a typical length of a test tube, in our analytical studies, we consider the tube to be infinite and take the spatial domain as $-\infty < x < +\infty$. Thus, we seek solutions of (16), (17) for $t > 0$, $-\infty < x < +\infty$ subject to the conditions

$$D(x,0) = 0, \quad \eta(x,0) = H(-x), \tag{20}$$

$$\eta(x,t) = 1 \ \text{ as } x \to -\infty, \quad \frac{\partial \eta(x,t)}{\partial x} = 0 \ \text{ as } x \to \infty. \tag{21}$$

Note that the x_o introduced earlier is equal to zero. Introducing two-timing with a fast time scale t and a slow scale $\tau = \varepsilon t$ (with $\varepsilon \ll 1$), we can write the system

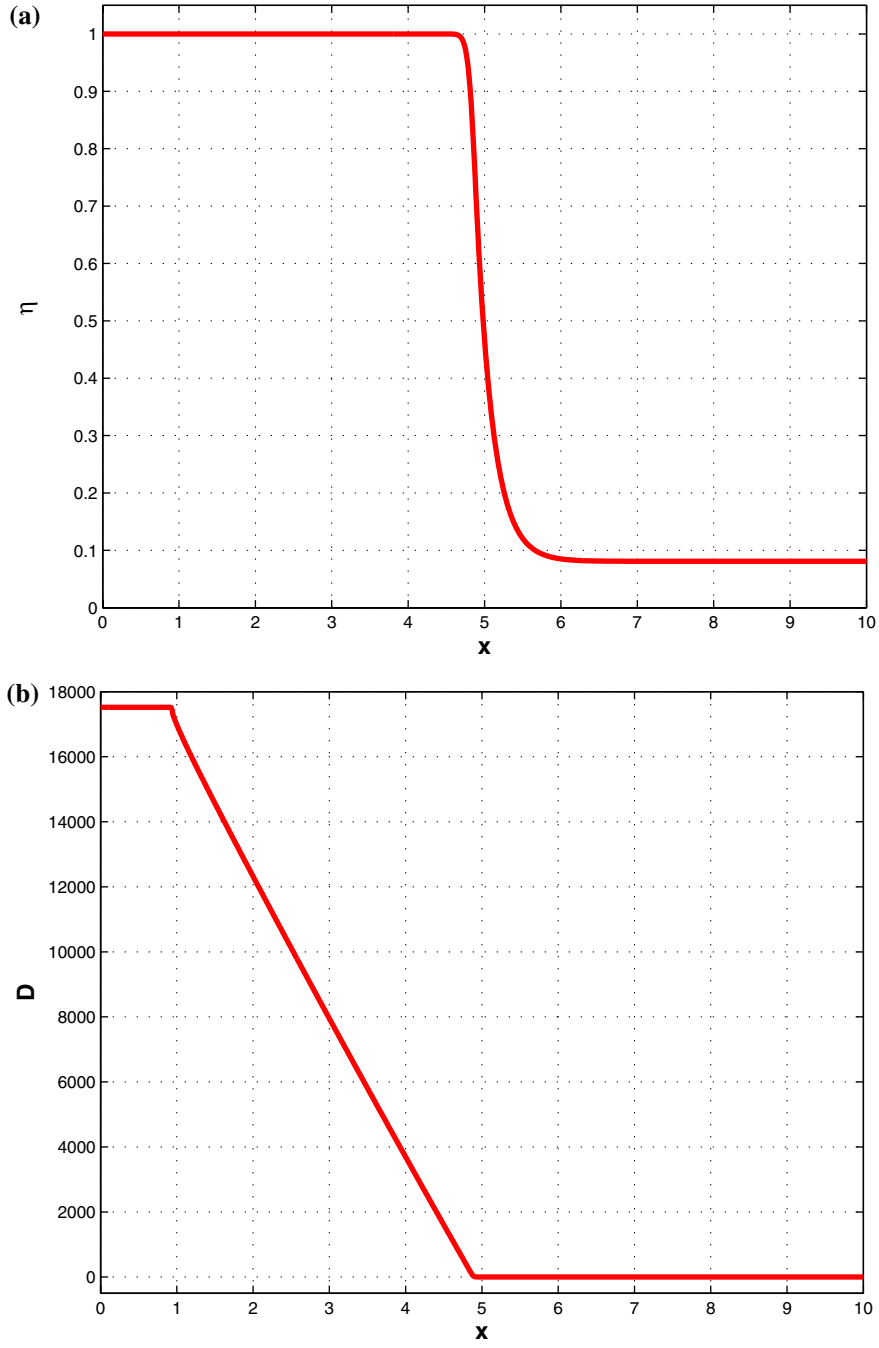

Figure 2. The plots display the spatial profiles of the degree of conversion of monomers and the concentration of radicals, respectively, at a fixed time over the full interval.

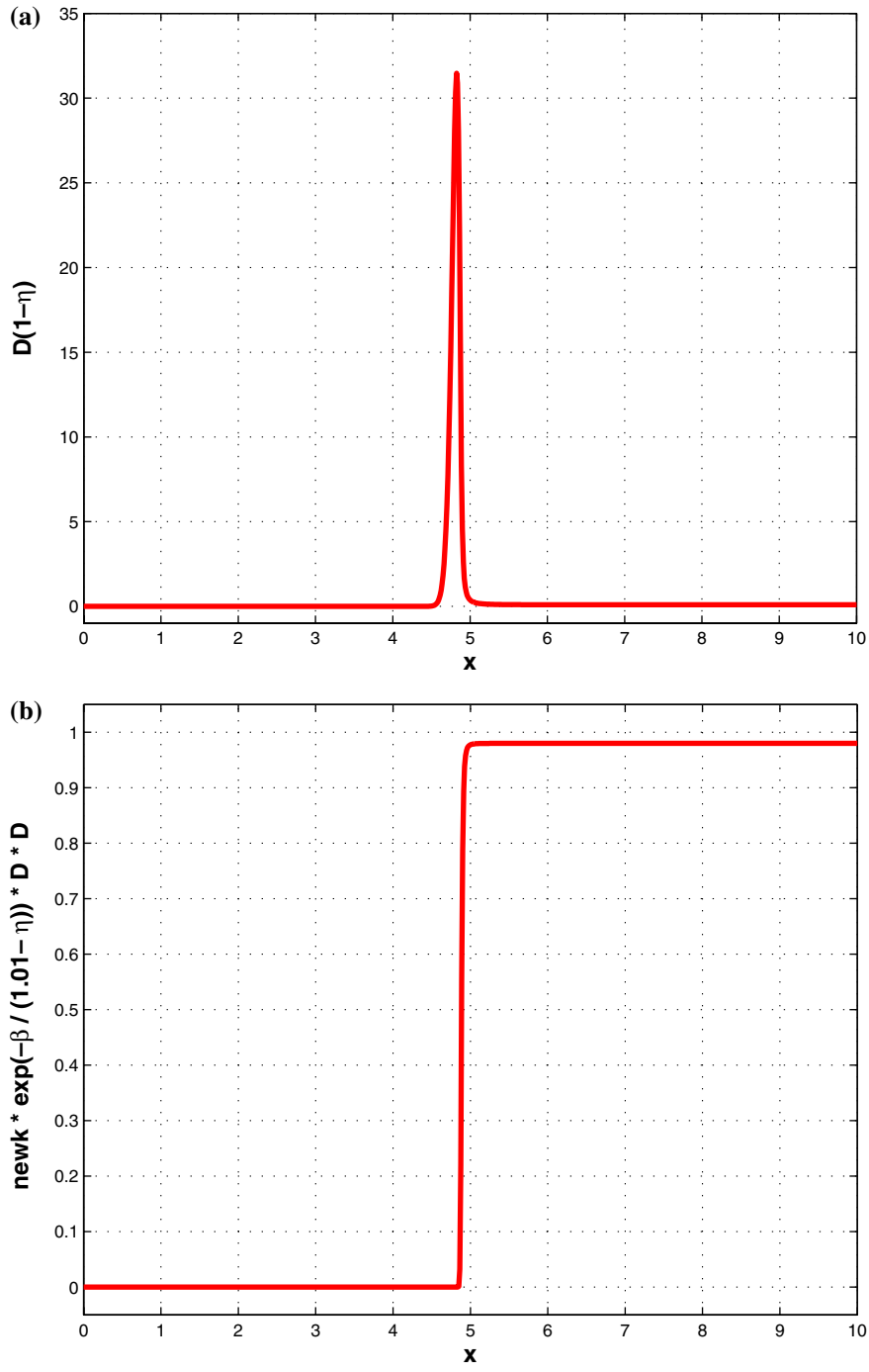

Figure 3. The plots display the spatial profiles of the reaction term and the rate of termination of radical (quantified by the last term of equation (16)), respectively, at a fixed time over the full interval.

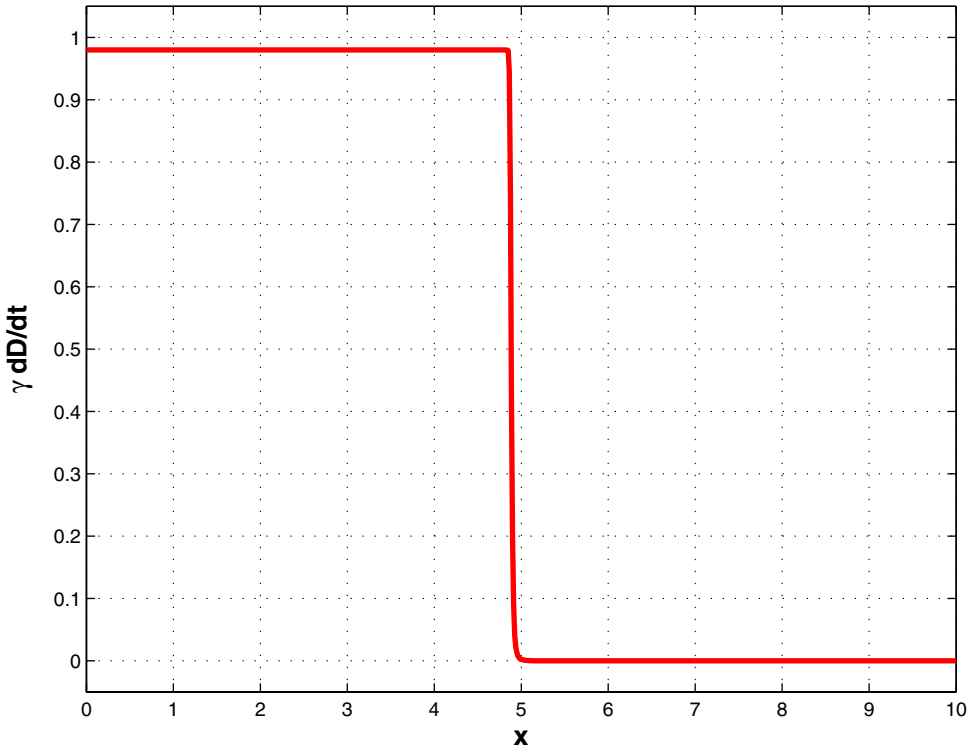

Figure 4. The plot displays the spatial profile of the rate of change of the concentration of radicals (quantified by the first term of equation (16)) at a fixed time over the full interval.

Table 2
Parameter values for the PMMA/MAA system with AIBN as initiator.

Parameter	Values	
k_d	$1.45 \cdot 10^{-6}$	1/s
k_p	522	l/(mol·s)
k_t	$4.82 \cdot 10^{11}$	l/(mol·s)
I_o	0.001	mol/l
M_o	9.0	mol/l
D_M	$1 \cdot 10^{-6}$	cm^2/s
f	0.5	
β	5	
ε	$2.27 \cdot 10^{-2}$	
γ	$1.02 \cdot 10^{-5}$	
k	$9.82 \cdot 10^4$	

(16), (17), (20), (21) in the form

$$\gamma\left(\frac{\partial D}{\partial t}+\varepsilon\frac{\partial D}{\partial \tau}\right)=\mathrm{e}^{-\varepsilon t}-k\,\mathrm{e}^{\frac{-\beta}{1-\eta}}D^2, \tag{22}$$

$$\frac{\partial \eta}{\partial t}+\varepsilon\frac{\partial \eta}{\partial \tau}=\frac{\partial^2\eta}{\partial x^2}+D\,(1-\eta)\,, \tag{23}$$

$$D(x,0,0)=0,\quad \eta(x,0,0)=H(-x), \tag{24}$$

$$\eta(x,t,\tau)=1\ \text{ as } x\to-\infty,\quad \frac{\partial\eta(x,t,\tau)}{\partial x}=0\ \text{ as } x\to\infty. \tag{25}$$

We seek a solution to leading order in ε.

4.2.1. Bulk polymerization

We first discuss the polymerization process in the bulk region, far from the reaction zone as $x\to+\infty$. Here we seek the value of the degree of conversion η_b and the radical concentration D_b as a function of slow time τ. These limiting values of the concentrations do not depend on x so we can set $\partial^2\eta/\partial x^2=0$ in (23). We also apply the steady-state assumption [14] which corresponds to setting the time derivatives in equation (22) to zero. In explanation, the highly reactive radicals in the bulk are consumed as fast as they are created. Hence the rate balance for D is assumed to be zero. Implementing these assumptions to the system (22)–(25) results in the following initial value problem:

$$\mathrm{e}^{-\tau}=k\mathrm{e}^{\frac{-\beta}{1-\eta_b}}D_b^2, \tag{26}$$

$$\varepsilon\frac{\mathrm{d}\eta_b}{\mathrm{d}\tau}=D_b\,(1-\eta_b)\,,\quad \eta_b(0)=0. \tag{27}$$

We solve equation (26) for D_b and substitute the result into equation (27) to obtain

$$\varepsilon\frac{\mathrm{d}\eta_b}{\mathrm{d}\tau}=\mathrm{e}^{\tau/2}\frac{1}{\sqrt{k}}\,\exp\left(\frac{\beta/2}{1-\eta_b}\right)\,(1-\eta_b)\,. \tag{28}$$

By separating variables in (28) and integrating, we obtain

$$\int_0^{\eta_b}\frac{\exp\left(\frac{-\beta/2}{1-\eta}\right)}{1-\eta}\mathrm{d}\eta=\frac{1}{\varepsilon\sqrt{k}}\int_0^{\tau}\mathrm{e}^{-\tau/2}\mathrm{d}\tau.$$

Making the change of variable $\xi=\frac{\beta/2}{1-\eta}$ in the first integral gives

$$\int_{\beta/2}^{\frac{\beta/2}{1-\eta_b}}\frac{\mathrm{e}^{-\xi}}{\xi}\,\mathrm{d}\xi=\frac{1}{\varepsilon\sqrt{k}}\int_0^{\tau}\mathrm{e}^{-\tau/2}\mathrm{d}\tau.$$

We can determine the time, τ_f, needed for the reaction to come to completion (that is, when the monomer is completely consumed by the reaction), by applying the limit $\eta_b \to 1$ to get

$$E_1\left(\frac{\beta}{2}\right) = \frac{2}{\varepsilon\sqrt{k}}\left(1 - \mathrm{e}^{-\tau_f/2}\right), \tag{29}$$

where

$$E_1(z) \equiv \int_z^\infty \frac{\mathrm{e}^{-r}}{r}\,\mathrm{d}r,$$

is known as the exponential integral [20]. For sufficiently large β the left-hand side of (29) is small. Thus, the right-hand side of (29) and, therefore, τ_f must be small. Expanding the exponential for small τ_f yields the completion time as

$$\tau_f \approx \varepsilon\sqrt{k}\; E_1\left(\frac{\beta}{2}\right).$$

There is also a lower limit for β under which the reaction stops not due to the complete consumption of the monomer, but of the initiator and deemed as "initiator burnout". This case corresponds to an "infinite" time of completion τ_f. Taking the limit $\tau_f \to \infty$ in (29), we observe that β must be greater than β_* determined by

$$\frac{\varepsilon\sqrt{k}}{2} E_1\left(\frac{\beta_*}{2}\right) = 1.$$

For the base parameter values in Table 2 we obtain $\beta_* = 1.71$.

4.2.2. Frontal polymerization

We now return to the system (22)–(25). We seek a solution in the form of a slowly-varying right traveling wave and introduce a moving coordinate system

$$z = x - \int_0^t c\,\mathrm{d}s,$$

where the nondimensional propagation speed $c = c(\varepsilon t)$ is a function of the slow time, and the front is always located at $z = 0$. The leading order in small ε solution of (22)–(23), for which we retain the notation $\eta(z,\tau)$ and $D(z,\tau)$, satisfies the system of equations

$$-\gamma c(\tau)\frac{\mathrm{d}D}{\mathrm{d}z} = \mathrm{e}^{-\tau} - k\mathrm{e}^{\frac{-\beta}{1-\eta}}D^2, \quad D(+\infty) = D_b, \tag{30}$$

$$\frac{\mathrm{d}^2\eta}{\mathrm{d}z^2} + c(\tau)\frac{\mathrm{d}\eta}{\mathrm{d}z} + D\,(1-\eta) = 0, \quad \eta(-\infty) = 1, \quad \eta(+\infty) = \eta_b. \tag{31}$$

Numerical results suggest the direction to take to approximate an analytic solution. Figures 2–4 show various plots of the solution to the full problem (equations (16)–(19)). Since some of the graphs exhibit rapid variations over a certain spatial region, we show in figures 5–7 the corresponding stretched spatial region.

First, we observe that the reaction zone (figure 6(a)) is narrow compared to the scale of variation of η (figure 5(a)). The reaction zone consists of two parts: left and right of the maximum value. The right part of the reaction zone is shorter than the left part thus introducing the smallest spatial scale in the problem. Next, there is an important change in the behavior of D (figure 5(b)) that occurs over the right part of the reaction zone. This change can be attributed to a change in the relative significance of the terms in equation (30). Figures 6(b) and 7 indicate that to the right of the reaction zone, the dominant balance in (30) is due to the second and third terms of the equation (which simply means that the steady state approximation is applicable in this region). In the left part of the reaction zone, the dominant balance is due to the first and second terms of the equation (the termination rate is negligible due to the gel effect, so a linear growth of the radical concentration is observed). Since the scale of the right part of the reaction zone is the smallest, in our approximation of the solution, we shrink it to a point. Since the problem is invariant with respect to translations in z, we will take this point to be $z = 0$. To the right of this point, we solve a reactionless equation for η and use the steady state approximation in the D-equation. To the left of this point, we use the other simplification of the D-equation. Thus, we solve the following problem. For $z > 0$, we solve

$$0 = \mathrm{e}^{-\tau} - k\mathrm{e}^{\frac{-\beta}{1-\eta}} D^2, \tag{32}$$

$$\frac{\mathrm{d}^2\eta}{\mathrm{d}z^2} + c(\tau)\frac{\mathrm{d}\eta}{\mathrm{d}z} = 0 \tag{33}$$

subject to the boundary condition

$$\eta(+\infty) = \eta_b.$$

For $z < 0$, we solve

$$-\gamma c(\tau)\frac{\mathrm{d}D}{\mathrm{d}z} = \mathrm{e}^{-\tau}, \tag{34}$$

$$\frac{\mathrm{d}^2\eta}{\mathrm{d}z^2} + D\,(1-\eta) = 0 \tag{35}$$

subject to the boundary condition

$$\eta(-\infty) = 1.$$

Note that the first derivative term is omitted in equation (35); as the left part of the reaction zone is narrow, the second derivative term is more important than

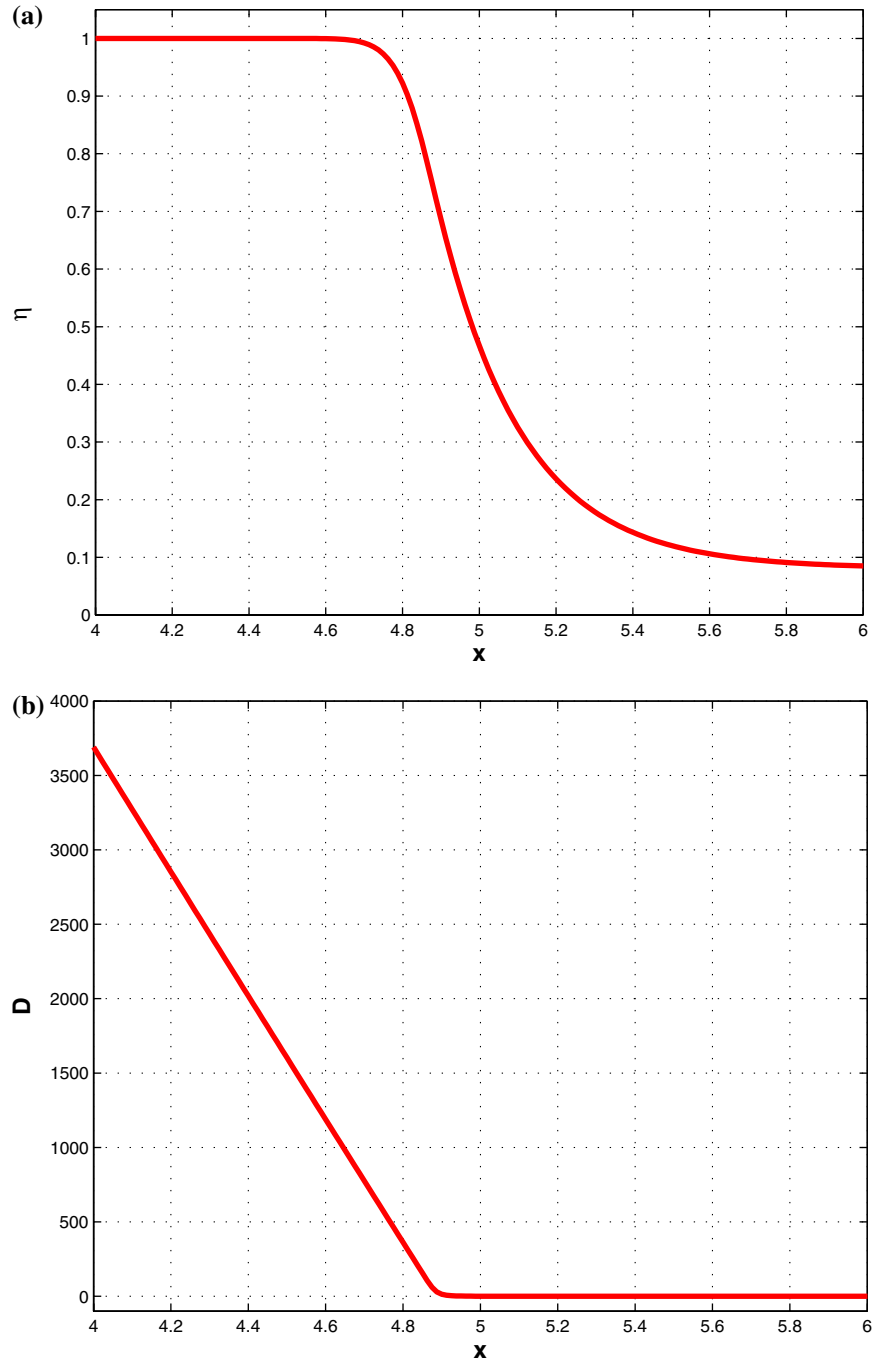

Figure 5. The plots display the spatial profiles of the degree of conversion of monomers and the concentration of radicals, respectively, at a fixed time over a stretched spatial region.

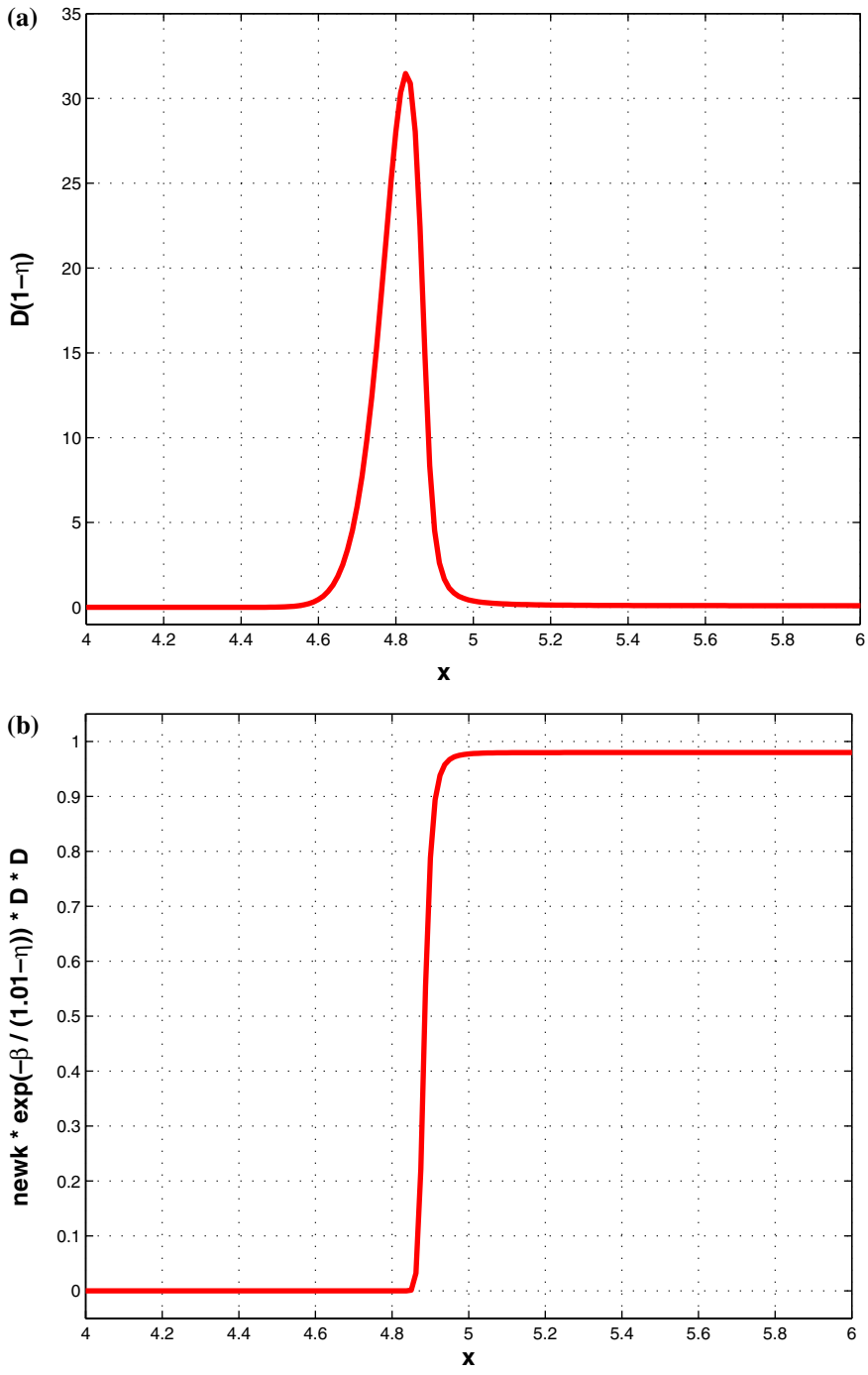

Figure 6. The plots display the spatial profiles of the reaction term and the rate of termination of radical (quantified by the last term of equation (16)), respectively, at a fixed time over a stretched spatial region.

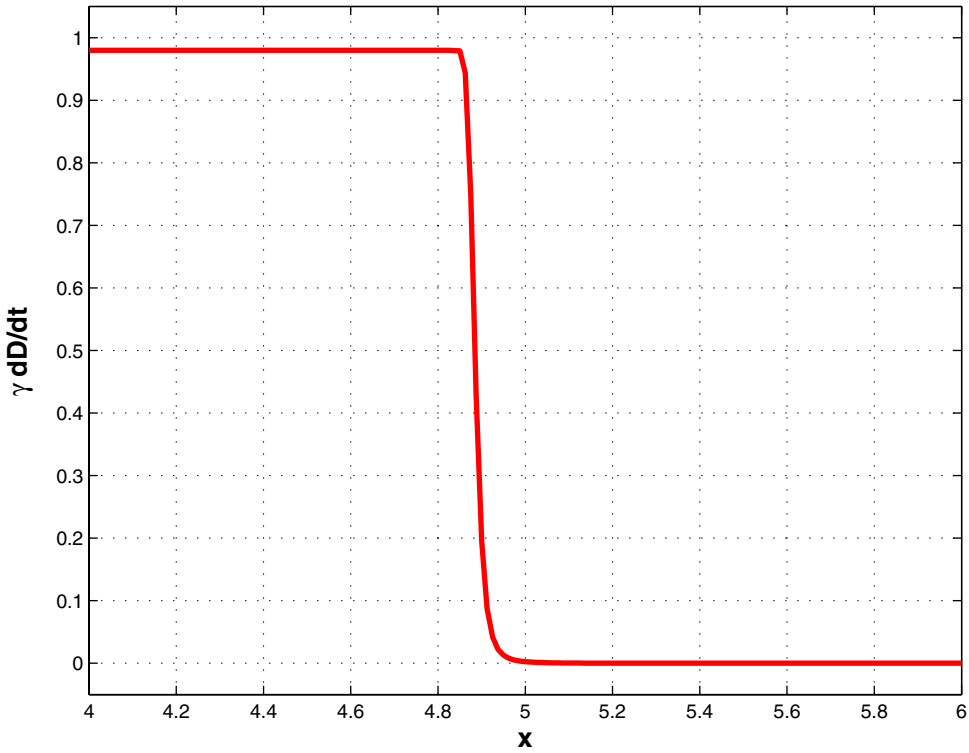

Figure 7. The plot displays the spatial profile of the rate of change of the concentration of radicals (quantified by the first term of equation (16)) at a fixed time over a stretched spatial region.

the first derivative term. We match these solutions at $z = 0$ in such a way that D, η and $\mathrm{d}\eta/\mathrm{d}z$ are all continuous. An additional condition that we impose on the solution is that the maximum value of the reaction rate is attained at $z = 0$, i.e.,

$$\frac{\mathrm{d}}{\mathrm{d}z}[D\,(1-\eta)]|_{z=0^-} = 0. \tag{36}$$

Introducing the notation

$$\eta(0) = \eta_*, \quad D(0) = D_*, \tag{37}$$

where η_* and D_* are two unknown quantities related by

$$\mathrm{e}^{-\tau} = k\mathrm{e}^{\frac{-\beta}{1-\eta_*}} D_*^2 \tag{38}$$

(see (32)), we obtain upon solving (32)–(35)

$$\eta(z) = \begin{cases} \eta_b + (\eta_* - \eta_b)\mathrm{e}^{-cz}, & z > 0 \\ 1 - (1-\eta_*)\mathrm{Ai}(\alpha D_* - \alpha^{-1/2} z)/\mathrm{Ai}(\alpha D_*), & z < 0 \end{cases}, \tag{39}$$

$$D(z) = \begin{cases} \gamma \mathrm{e}^{-\tau} \mathrm{e}^{\beta/(1-\eta(z))}, & z > 0 \\ D_* - \alpha^{-3/2} z, & z < 0 \end{cases}, \tag{40}$$

where Ai is the Airy function and

$$\alpha = (\gamma c \mathrm{e}^{\tau})^{2/3}. \tag{41}$$

To derive the solutions (39) and (40), we used the boundary conditions at $\pm\infty$ and the continuity conditions for η and D at $z = 0$. The remaining matching condition, which constitutes the continuity of $\mathrm{d}\eta/\mathrm{d}z$ at $z = 0$ takes the form

$$(1-\eta_*)\alpha^{-1/2} \frac{\mathrm{Ai}'(\alpha D_*)}{\mathrm{Ai}(\alpha D_*)} = -c(\eta_* - \eta_b). \tag{42}$$

Thus, we have three equations (36), (38), and (42) for the three unknowns: η_*, D_* and c.

Substituting the solution for η and D into (36), we obtain upon some simplifications

$$\mathrm{Ai}(\alpha D_*) + \alpha D_* \mathrm{Ai}'(\alpha D_*) = 0, \tag{43}$$

from which

$$\alpha D_* \approx 0.9. \tag{44}$$

Using (43), (44) we reduce (42) to

$$(1-\eta_*)\alpha^{-1/2} = 0.9c(\eta_* - \eta_b). \tag{45}$$

Substituting D_* found from equation (38) in terms of η_*, and α given by (41) into (44) and (45), we obtain

$$1 - \eta_* = 0.9c(\eta_* - \eta_b)(\gamma c \mathrm{e}^{\tau})^{1/3}, \tag{46}$$

$$\left[\gamma \mathrm{e}^{-\tau} \mathrm{e}^{\frac{\beta}{1-\eta_*}}\right]^{1/2} = (\gamma c \mathrm{e}^{\tau})^{-2/3}. \tag{47}$$

Thus, the problem has boiled down to solving the two equations (46) and (47) for the two unknowns c and η_*. Upon simple manipulations we obtain an equation for c in terms of η_* and an equation for η_*

$$c = \frac{1}{\gamma^{1/4}} \left(\frac{1-\eta_*}{\eta_* - \eta_b}\right)^{3/4} \mathrm{e}^{-\tau/4}, \tag{48}$$

$$\frac{1-\eta_*}{\eta_* - \eta_b} = 0.7 \frac{1}{\gamma^2} \mathrm{e}^{-\frac{\beta}{1-\eta_*}}. \tag{49}$$

An approximate solution of equation (49) for η_* has the form

$$\eta_* = 1 - \frac{\beta}{2\ln\frac{1}{\gamma} + \ln\left(\frac{2}{\beta}\ln\frac{1}{\gamma}\right)},$$

which, upon substitution in (48), yields

$$c = \frac{1}{\gamma^{1/4}}\left(\frac{\beta}{(1-\eta_b)\left[2\ln\frac{1}{\gamma} + \ln\left(\frac{2}{\beta}\ln\frac{1}{\gamma}\right)\right] - \beta}\right)^{3/4} e^{-\tau/4}. \tag{50}$$

5. Discussion

As we can see from (50), the speed of the wave depends on the termination rate parameters, in particular on β. Specifically, the steeper it is (so β increases), the faster it moves. The wave front moves to the right with a velocity of about $\beta^{3/4}$.

Figure 8 shows the propagation velocity of the wave as a function of β using analytic results and numerical simulations. Also shown within each figure is a comparison of the velocity for varied γ values. Observe in (50) that $c \propto \gamma^{-1/4}$, that is, the velocity decreases with increasing γ. The graphs demonstrate the accuracy of the analytical approximations. The general trends of the analytical results qualitatively match the numerical solution of the full problem for the propagation velocity and further imply that they are consistent with any assumptions or approximations taken.

In figure 9 we graph the propagation velocity as a function of time for various γ values. The curves shows that the propagation velocity of the polymerization wave is mainly constant. But there is a slight increase in the velocity for increasing γ, as shown in figure 9.

6. Mathematical model with inhibition

6.1. Basic mechanism

As discussed earlier, the breakdown of a propagating front occurs due to bulk polymerization. In order to affect the polymerization in the bulk, an inhibitor species can be added to the initial mixture. The inhibitor reacts with growing polymer chains terminating polymerization. Thus, the inhibitor slows down bulk polymerization, letting the front propagate longer. On the other hand, if the inhibitor is able to penetrate the front, it affects the reactions at the front and slows down the front. Below we consider the situation in which small amount of a strong inhibitor (that is able to penetrate the front) is added to the initial mixture.

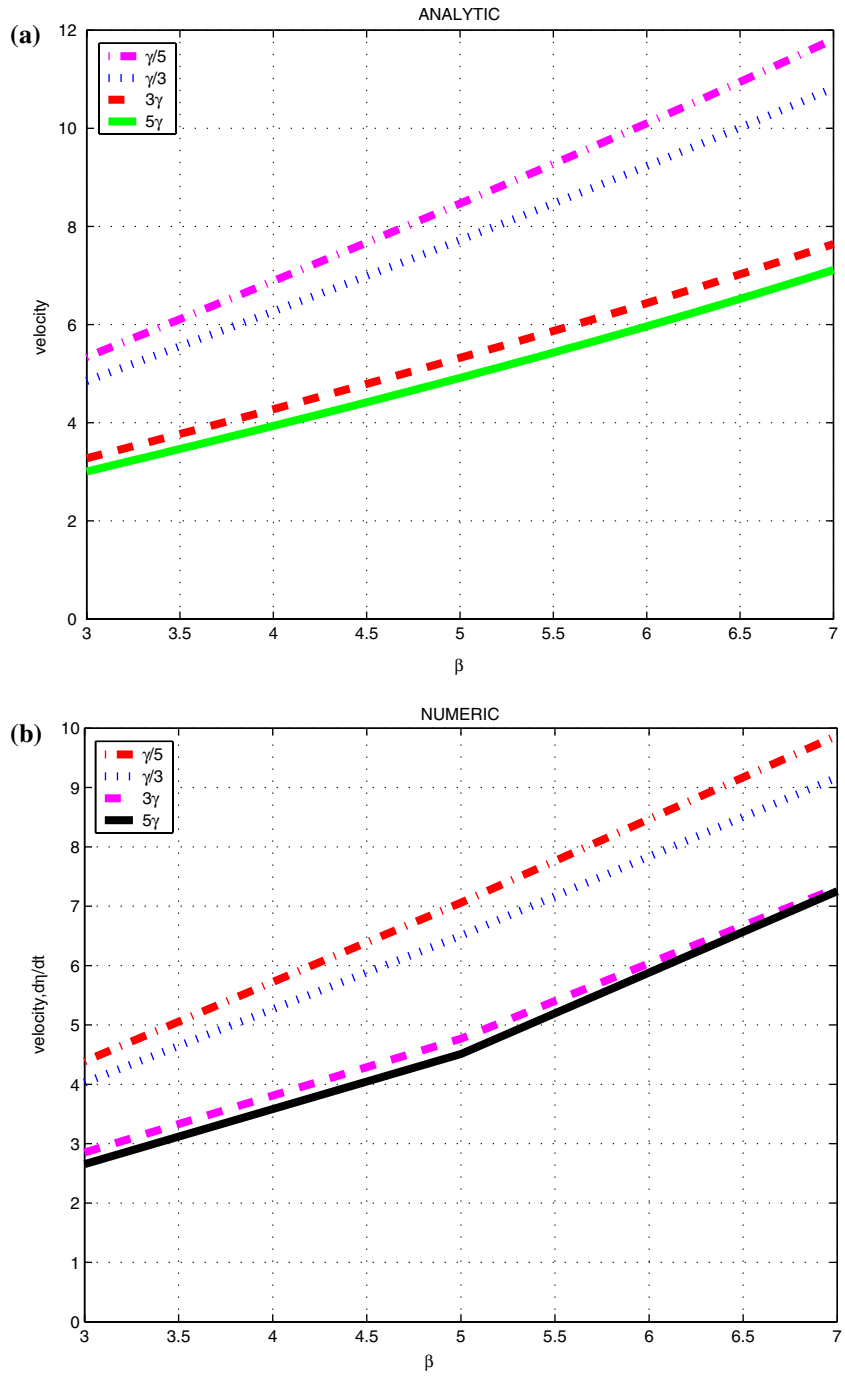

Figure 8. Nondimensional analytical and numerical propagation velocity of the polymerization wave as a function of β for various γ. The top curves correspond to the smallest γ values.

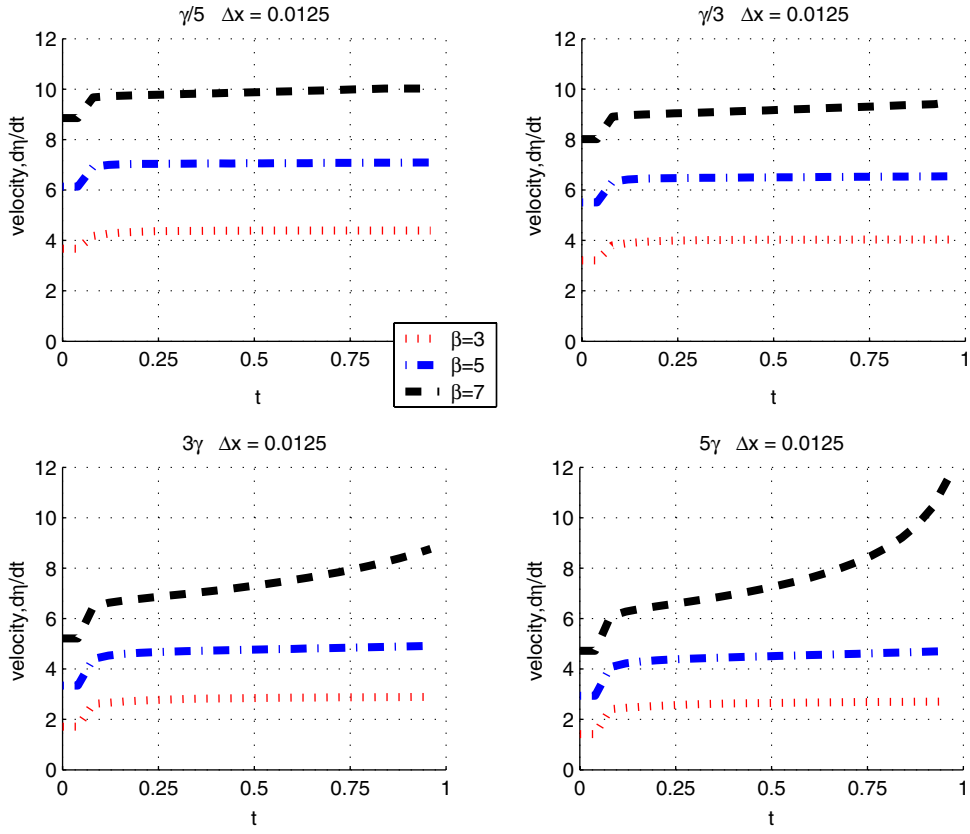

Figure 9. Nondimensional propagation velocity of the polymerization wave as a function of time for various γ. The top curves correspond to the smallest β values.

We again consider the kinetic scheme summarizing IFP as given in Section 2.1, but now adding an inhibition reaction

$$\text{Initiation} \begin{cases} I \xrightarrow{k_d} f\ 2R\cdot \\ R\cdot + M \xrightarrow{k_i} P_1\cdot \end{cases}$$

$$\text{Propagation} \begin{cases} P_1\cdot + M \xrightarrow{k_p} P_2\cdot \\ P_2\cdot + M \xrightarrow{k_p} P_3\cdot \\ \quad\cdots \\ P_j\cdot + M \xrightarrow{k_p} P_{j+1}\cdot \\ \quad\cdots \end{cases}$$

$$\text{Termination} \left\{ P_n \cdot + P_m \cdot \xrightarrow{k_{tg}} P \right.$$

$$\text{Inhibition} \left\{ P_n \cdot + S \xrightarrow{k_s} Y \right.$$

Here S denotes the inhibitor species, Y the product(s) of the inhibition reaction (being either nonradical species or radicals of reactivity too low to undergo propagation), and k_s the reaction rate for the inhibition chemical equation.

The corresponding system of equations is

$$\frac{\partial \tilde{I}}{\partial \tilde{t}} = -k_d \tilde{I} \tag{51}$$

$$\frac{\partial \tilde{D}}{\partial \tilde{t}} = 2 f k_d \tilde{I} - 2 k_{tg} \tilde{D}^2 - k_s \tilde{D} \tilde{S} \tag{52}$$

$$\frac{\partial \tilde{M}}{\partial \tilde{t}} = D_M \frac{\partial^2 \tilde{M}}{\partial \tilde{x}^2} - k_p \tilde{D} \tilde{M} \tag{53}$$

$$\frac{\partial \tilde{P}}{\partial \tilde{t}} = k_{tg} \tilde{D}^2 \tag{54}$$

$$\frac{\partial \tilde{S}}{\partial \tilde{t}} = -k_s \tilde{D} \tilde{S} \tag{55}$$

$$\frac{\partial \tilde{Y}}{\partial \tilde{t}} = k_s \tilde{D} \tilde{S} \tag{56}$$

with initial conditions

$$\tilde{I}(\tilde{x}, 0) = I_o, \quad \tilde{M}(\tilde{x}, 0) = M_o \cdot H(\tilde{x} - x_o), \quad \tilde{S}(\tilde{x}, 0) = S_o,$$
$$\tilde{D}(\tilde{x}, 0) = 0, \quad \tilde{P}(\tilde{x}, 0) = 0, \quad \tilde{Y}(\tilde{x}, 0) = 0$$

and boundary conditions for the monomer concentration as

$$\tilde{M}(0, \tilde{t}) = 0, \quad \frac{\partial \tilde{M}(L, \tilde{t})}{\partial \tilde{x}} = 0.$$

Thus, we assume that the inhibitor and initiator are uniformly distributed in the initial mixture. And as before, we fill in the region $0 < \tilde{x} < x_o$ with a polymer substrate which is free of monomer, while the remaining part $x_o < \tilde{x} < L$ of the initial mixture is filled with monomer. The above system is derived in the same manner as equations (3a)–(3d) using the same simplifying assumptions as in Section 2.1, and the definition of the termination rate is as given in Section 2.3. As before, because the current study is not concerned with the product states, we only study equations (51)–(53) and (55), but if needed, can determine the products once $\tilde{D}$ and $\tilde{S}$ are determined. As was in the case for the noninhibited polymerization process, $\tilde{I}$ can be solved for explicitly in (51) and substituted into (52).

6.2. Nondimensionalization

Using the same nondimensional quantities as before and also including

$$S = \frac{\tilde{S}}{S_o}, \quad Z = \frac{k_s}{k_p}, \quad \lambda = \frac{\gamma Z S_o}{D_*}$$

we obtain from equations (51)–(56) the nondimensional system

$$\gamma \frac{\partial D}{\partial t} = \mathrm{e}^{-\varepsilon t} - k\mathrm{e}^{\frac{-\beta}{1-\eta}} D^2 - \lambda DS \tag{57}$$

$$\frac{\partial \eta}{\partial t} = \frac{\partial^2 \eta}{\partial x^2} + D(1-\eta) \tag{58}$$

$$\frac{\partial S}{\partial t} = -ZDS \tag{59}$$

$$D(x,0) = 0, \quad \eta(x,0) = H(x_o - x),$$
$$S(x,0) = 1, \quad \eta(0,t) = 1, \quad \frac{\partial \eta(L,t)}{\partial x} = 0. \tag{60}$$

The potential for the inhibition of polymerization is inherent in the parameters Z and S_o. Here Z, the ratio of inhibition rate to the propagation rate, is a nondimensional measure of the strength of the inhibitor; if $Z \gg 1$, for example, we say the inhibitor is strong. S_o is the dimensional initial concentration of the inhibitor. An inhibitor that is strong yet present in too small of an amount will suppress the polymerization for only a very short period of time. On the other hand, an inhibitor that is weak yet abundant in its concentration may retard the polymerization for a longer period of time, but less effectively. The numerical values of Z depend on the choice of inhibitor and are experimentally known. A commonly used strong inhibitor is oxygen, with $Z = 33000$. Note that in the case $Z = 0$, the system is reduced to the one without inhibition and discussed in the previous sections.

The appearance of the parameter λ present in equation (57) pertains to the consumption of the radicals due to inhibition. Note that it is proportional to Z. In the right hand side of (57), the first term describes the rate of creation of D (which is equal to the rate of decomposition of the initiator I), and second and third terms describe the rate of annihilation of D, either by termination or inhibition, respectively. The evolution of η is given by equation (58) and the consumption of the inhibitor is given by equation (59). Hence, equations (57)–(60) and the parameters discussed above complete our formulation of the problem.

6.3. Numerical results

Following similar analysis to the case without inhibition, we use the Method of Lines to get the numerical solution of the reduced problem

(57)–(60). In Figure 10, the degree of conversion profiles at selected times are shown.

Recall that figure 1 shows the numerical solution for the uninhibited system. In both cases, the increase in the degree of conversion ahead of the front indicates the existence of bulk polymerization. As anticipated, figure 10 shows the solution to have limited polymerization in the bulk. Hence, by adding an inhibitor to the system, polymerization of the monomer is suppressed, increasing the life-time of the propagating wave.

6.4. *Analytical results*

6.4.1. *Bulk Polymerization*

As before, we apply the steady state assumption to the radical equation and solve for S in closed form. We also neglect the diffusion term in the monomer

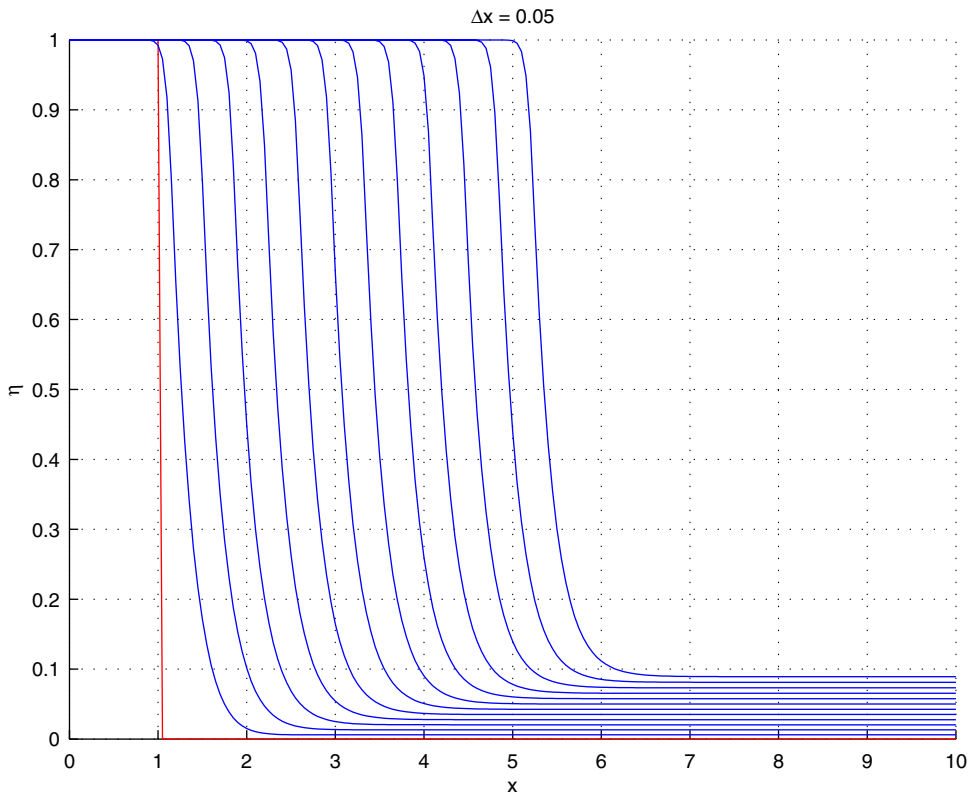

Figure 10. The curves display the spatial profile of the degree of conversion of the monomer at equally spaced values of time for a reaction with inhibitor.

equation to obtain

$$S_b = \frac{1}{\lambda D_b}\left(\mathrm{e}^{-\varepsilon t} - k\,\mathrm{e}^{\frac{-\beta}{1-\eta_b}} {D_b}^2\right) \tag{61}$$

$$\frac{\mathrm{d}\eta_b}{\mathrm{d}t} = D_b\,(1-\eta_b) \tag{62}$$

$$\frac{\mathrm{d}S_b}{\mathrm{d}t} = -Z D_b S_b \tag{63}$$

$$\eta_b(0) = 0, \quad S_b(0) = 1. \tag{64}$$

Upon substitution of (61) into equation (63), the evolution of the radicals can be written as

$$\frac{\mathrm{d}D_b}{\mathrm{d}t} = \frac{Z{D_b}^2\left(\mathrm{e}^{-\varepsilon t} - k\mathrm{e}^{\frac{-\beta}{1-\eta_b}} {D_b}^2\right) - \varepsilon \mathrm{e}^{-\varepsilon t} D_b + k\beta {D_b}^4 \mathrm{e}^{\frac{-\beta}{1-\eta_b}}/(1-\eta_b)}{\mathrm{e}^{-\varepsilon t} + k\mathrm{e}^{\frac{-\beta}{1-\eta_b}} {D_b}^2}. \tag{65}$$

Substituting the initial conditions (64) into equation (61) we obtain the initial condition for D_b:

$$D_b(0) = \frac{\lambda}{2k\mathrm{e}^{-\beta}}\left[\sqrt{1 + \frac{4k\mathrm{e}^{-\beta}}{\lambda^2}} - 1\right]. \tag{66}$$

The new governing system is given by (65) and (66) for the radicals, with the unchanged (62) and (64) for the degree of conversion. Next, we make the change of variables

$$D_b = \frac{1}{\sqrt{k}}\mathrm{e}^{\frac{\beta/2}{1-\eta_b}} y_b \tag{67}$$

motivated by the inhibition-free system in section 4.2.1. The radical concentration in the absence of inhibitor given by equation (26) is

$$D_b = \frac{1}{\sqrt{k}}\mathrm{e}^{\frac{\beta/2}{1-\eta_b}}\,\mathrm{e}^{-\varepsilon t/2}.$$

In the presence of inhibitor, the radical species can also react with the inhibitor molecules causing the polymerization reaction to terminate. Thus, we expect a decrease in the radicals so that for $Z = 0$ (no inhibition), $y_b = \mathrm{e}^{-\varepsilon t/2}$, while for $Z > 0$, $\quad y_b \leqslant \mathrm{e}^{-\varepsilon t/2}$.

By introducing the above change of variables (67) and a slow time scale $\tau = \varepsilon t$, the system of equations takes the form

$$\frac{dy_b}{d\tau} = -\frac{\beta/2}{\varepsilon(1-\eta_b)}\frac{e^{\frac{\beta/2}{1-\eta_b}}}{\sqrt{k}}{y_b}^2 + \frac{Z\frac{e^{\frac{\beta/2}{1-\eta_b}}}{\sqrt{k}}{y_b}^2\left(e^{-\tau}-{y_b}^2\right) - \varepsilon e^{-\tau}y_b + \beta\frac{e^{\frac{\beta/2}{1-\eta_b}}}{\sqrt{k}}{y_b}^4/(1-\eta_b)}{\varepsilon\left(e^{-\tau}+{y_b}^2\right)} \tag{68}$$

$$\frac{d\eta_b}{d\tau} = \frac{e^{\frac{\beta/2}{1-\eta_b}}}{\sqrt{k}}y_b\frac{1-\eta_b}{\varepsilon} \tag{69}$$

$$y_b(0) = \frac{\lambda e^{\beta/2}}{2\sqrt{k}}\left[\sqrt{1+\frac{4k}{\lambda^2 e^{\beta}}}-1\right] \equiv y_o \tag{70}$$

$$\eta_b(0) = 0 \tag{71}$$

The system (68)–(71) was solved numerically for several values of Z and β. The "reduced" radical concentration y_b as a function of the slow time is shown in figure 11 for $\beta = 5$ and various values of Z.

If $Z = 0$, then the solution follows the upper bound $y_b(\tau) = e^{-\tau/2}$, described previously. In this noninhibited system, the amount of radicals decrease steadily as radical species are consumed by the propagation step. For values of $Z \gg 1$, the solution shows a nonexistent or relatively small radical population initially but at some critical time indicates a sudden increase in the radical species. This is indicative of the effectiveness of the inhibitor as it reacts with the radical species and almost completely halts polymerization. At this critical point, the inhibitors are consumed and a front will be formed as the polymerization of the monomers resume. Past this critical value of time, the solution exhibits an asymptotic behavior toward the upper bound. When Z takes on intermediate values, the solution initially exhibits some increase in the radicals but eventually decays exponentially. This results from a weak inhibitor that retards the polymerization less effectively but for a longer period of time.

To necessitate strong inhibition we must have $Z \gg 1$. Hence, until otherwise stated, the following analysis is restricted for $Z \gg 1$. As suggested by the results in figure 11, there exists a critical time τ_o separating the inhibited and noninhibited regimes. Define τ_o to be the value of τ at which inhibition stops and propagation resumes, that is, the time when the inhibitor has been completely consumed. In order to determine an analytic value of τ_o, we make two assumptions based on numerical results to simplify the problem (68)–(71). First, note that for $\tau < \tau_o$, ${y_b}^2 \ll e^{-\tau}$ (see figure 11) and so we neglect ${y_b}^2$ as compared to $e^{-\tau}$. Second, for $\tau < \tau_o$, η_b is negligible, as the presence of inhibition implies no conversion of monomers.

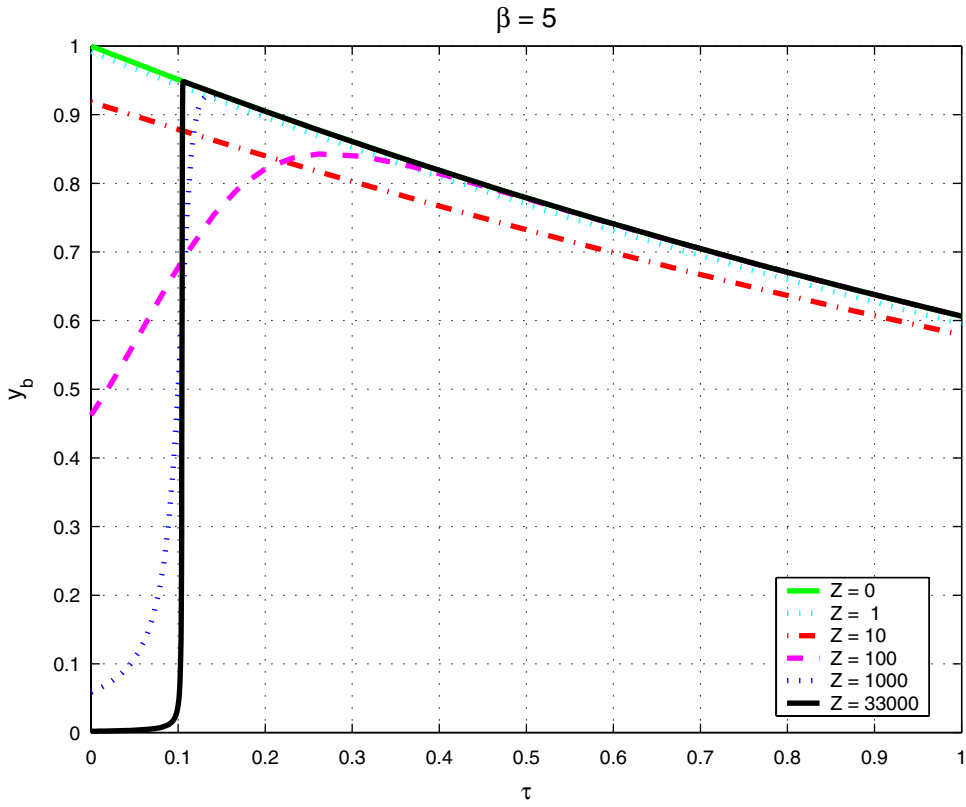

Figure 11. The plots display the nondimensional radical concentration profiles in the bulk region as a function of slow time for various Z. The reaction without inhibitor corresponds to the curve represented by $Z = 0$.

For $Z \gg 1$ and $\tau < \tau_o$, enforcing these simplifications into equations (68)–(71) yields the system of two equations, where one equation decouples from the other:

$$\frac{dy_b}{d\tau} = -\frac{\beta}{2}\frac{e^{\beta/2}}{\varepsilon\sqrt{k}}{y_b}^2 + Z\frac{e^{\beta/2}}{\varepsilon\sqrt{k}}{y_b}^2 - y_b + \beta\frac{e^{\beta/2}}{\varepsilon\sqrt{k}}{y_b}^4 e^{\tau}, \quad y_b(0) = y_o \tag{72}$$

$$\frac{d\eta_b}{d\tau} = \frac{e^{\beta/2}}{\varepsilon\sqrt{k}}y_b, \quad \eta_b(0) = 0. \tag{73}$$

Next, we further reduce the above equations by only keeping the terms which will substantially contribute to their solution. In particular, consider the right hand side of equation (72). In the inhibited region, figure 11 shows $y_b \ll 1$, and hence it follows that $y_b^4 \ll y_b^2$. Therefore, we neglect the last term on the right hand side of (72) as compared to the first term. Also, since we are under the assumption $Z \gg 1$, the value of $\beta/2$ is negligible compared to Z. This suggests

that the first term be neglected as compared to the second term. Applying these assumptions to equation (72) we obtain

$$\frac{dy_b}{d\tau} = ZK{y_b}^2 - y_b, \quad y_b(0) = y_o \tag{74}$$

where $K \equiv \frac{e^{\beta/2}}{\varepsilon\sqrt{k}}$. The solution of this problem is

$$y_b(\tau) = \frac{y_o}{ZKy_o + (1 - ZKy_o)e^{\tau}}. \tag{75}$$

Next, we can simplify the expression for y_o using the fact that $4k/(\lambda^2 e^{\beta}) \leqslant 1$ and expanding the square root to obtain

$$y_o = \frac{\lambda e^{\beta/2}}{2\sqrt{k}}\left[1 + \frac{1}{2}\frac{4k}{\lambda^2 e^{\beta}} + \cdots - 1\right] \approx \frac{\sqrt{k}}{\lambda e^{\beta/2}} = \frac{1}{Z\ K}\ \frac{2fI_o}{S_o} \tag{76}$$

$$= \frac{1}{Z}\frac{2\sqrt{fk_dk_tI_o}}{e^{\beta/2}k_pS_o} \equiv \frac{1}{Z}h. \tag{77}$$

Imposing the approximation (76) in the denominator and (77) in the numerator of solution (75), we get

$$y_b(\tau) = \frac{h/Z}{2fI_o/S_o + (1 - 2fI_o/S_o)e^{\tau}}. \tag{78}$$

Figure 11 shows a vertical asymptote of $y_b(\tau)$ as $\tau \to \tau_o$. This behavior is interpreted as the increase in radical concentration due to the end of the inhibition period. Setting the denominator of (78) to zero to obtain τ_o yields

$$\tau_o = -\ln\left[1 - \frac{S_o}{2fI_o}\right]. \tag{79}$$

An important observation should be made about (79). There is a critical value of the initial inhibitor concentration S_o given by $(S_o)_{cr} \equiv 2fI_o$. In the supercritical case, where $S_o > (S_o)_{cr}$, τ_o is undefined. The denominator of (78) remains positive and hence y_b monotonically decreases as time increases. In the critical case of $S_o = (S_o)_{cr}$, $y_b = 1/(ZK)$, a very small constant. Note that as $S_o \to (S_o)_{cr}$, then $\tau_o \to \infty$. This analysis reveals that large values of S_o assure that a strong inhibitor is never consumed. But the most interesting is the subcritical case where $S_o < (S_o)_{cr}$. We can approximate the step-like behavior (see figure 11) of the radicals by

$$y_b(\tau) = \begin{cases} y_o & \tau < \tau_o \\ e^{-\tau/2} & \tau > \tau_o \end{cases}. \tag{80}$$

For this subcritical case, the process of chemical conversion in the bulk is no longer negligible for $\tau > \tau_o$. Equations (69) and (71) can be reduced in this case using (80) to the initial value problem

$$\frac{d\eta_b}{d\tau} = \frac{e^{\frac{\beta/2}{1-\eta_b}}}{\varepsilon\sqrt{k}}(1-\eta_b)e^{-\tau/2}, \quad \eta_b(\tau_o) = 0. \tag{81}$$

Note that the above initial condition means that we take $\eta_b = 0$ for all $\tau < \tau_o$ due to negligible monomer conversion during the inhibition period. We can now determine at what time τ_f the reactions will stop. In this case, it occurs due to the full conversion of monomers. Separating variables in (81) and integrating from $\tau = \tau_o$, $\eta_b = 0$ to $\tau = \tau_f$, $\eta_b = 1$ we obtain

$$E_1\left(\frac{\beta}{2}\right) = \frac{2}{\varepsilon\sqrt{k}}\left(e^{-\tau_o/2} - e^{-\tau_f/2}\right). \tag{82}$$

Hence, for large β, we can write

$$\tau_f \approx \varepsilon\sqrt{k}E_1\left(\frac{\beta}{2}\right).$$

A lower bound can be established on β. From (82)

$$\frac{\varepsilon\sqrt{k}}{2}E_1\left(\frac{\beta}{2}\right) \leqslant 1$$

and, solving for β in this inequality, we numerically determine the lower bound as $\beta \geqslant 1.71$. Similar to the inhibition-free study, if values of β smaller than the numerical lower bound are chosen, then the reaction stops due to the "burnout" of the initiator. That is, polymerization is quenched due to the complete consumption of the initiators, and gel effect in the bulk region never occurs.

6.4.2. Frontal polymerization

Adding a small amount of a strong inhibitor to the system simply delays the process of polymerization by time τ_o and modifies the initial initiator concentration. Otherwise, our results on frontal polymerization without inhibition, discussed in Section 4.2.2, hold.

7. Conclusion

In this paper we discuss the propagation of an isothermal polymerization front due to coupling of the gel effect and mass diffusion of the monomer. The gel effect is modeled via a dependence of the termination rate on the degree of

conversion of the monomer. In the previous work [4] this dependence was modeled in an ad hoc fashion by using a step-wise function. Here we use the experimental data in [13,16] and free volume theory approach [17,18] to derive the dependence of the termination rate on the degree of conversion.

The qualitative behavior of the front was successfully modeled as shown by the numerical solution of the full problem. The main features of the solution are the appearance of slowly-varying traveling waves and a possible breakdown of the front due to bulk polymerization. The systems with and without an inhibitor have been considered. The main effect of a strong inhibitor present in small amounts is a delay in formation of the polymerization front.

Quantitative characteristics of the model, such as the propagation velocity of the front was calculated using analytical procedures. Comparison of the analytical and numerical results is satisfying.

Acknowledgment

This research has been supported in part by NSF grants DMS-0103856 and CTS-0138712.

References

[1] M.F. Perry and V.A. Volpert, J. Eng. Math. 49 (2004) 359.
[2] B. Smirnov, S.S. Minko, I. Lusinov, A. Sidorenko, E. Stegno and V. Ivanov, Polym. Sci. 35 (1993) 423.
[3] V. Golubev, D. Gromov and B. Korolev, J. Appl. Polym. Sci. 46 (1992) 1501.
[4] C. Spade and V. Volpert, Mathematic. Comp. Model. 30 (1999) 67.
[5] C. Spade and V. Volpert, Macromol. Theory Simul. 9 (2000) 26.
[6] D. A. Schult, C. A. Spade and V. A. Volpert, Appl. Mathematics Lett. 15 (2002) 749.
[7] V. Ivanov and E. Stegno, Polym. Sci. Ser. B 37 (1995) 50.
[8] V. Ivanov, E. Stegno and L. M. Pushchaeva, Chem. Phys. Rep. 16 (1997) 947.
[9] J. Masere, L. Lewis and J. Pojman, J. Appl. Polym. Sci. 80 (2001) 686.
[10] L. Lewis, C. DeBisschop, J.A. Pojman and V. Volpert, in: *Nonlinear Dynamics in Polymeric Systems*, eds. J. Pojman and Q. Tran-Cong-Miyata (American Chemical Society, Washington, DC, 2003), pp. 69–183.
[11] V. Ivanov, E. Stegno and L.M. Pushchaeva, Polym. Sci. Ser. A 44 (2002) 1017.
[12] Y. Koike, in: *Polymers for Lightwave and Integrated Optics*, ed. L.A. Hornak (Marcel Dekker, New York, 1992), pp. 71–104.
[13] B.P. Chekal, Understanding the Roles of Chemically-Controlled and Diffusion-Limited Processes in Determining the Severity of Autoacceleration Behavior in Free Radical Polymerization, Ph.D. thesis, Northwestern University (2002).
[14] G. Odian, *Principles of Polymerization, 2nd edition*, (Wiley-Interscience, New York, 1981).
[15] C. Spade and V. Volpert, Chem. Eng. Sci. 55 (2000) 641.
[16] B.P. Chekal and J.M. Torkelson. Macromolecules 35 (2002) 8126.
[17] J.S. Vrentas and J.L. Duda, J. Polym. Sci. Pol. Phys. 15 (1977) 403.
[18] J.S. Vrentas and J.L. Duda, J. Polym. Sci. Pol. Phys. 15 (1977) 417.

[19] J. Brandrup and E. Immergut, *Polymer Handbook* (John Wiley and Sons, New York, NY, 1982).
[20] M. Abramowitz and I.A. Stegun, *Handbook of Mathematical Functions*, (National Bureau of Standards, 1964).